Electronic Supplementary Material (ESI) for Soft Matter.

Supplementary material A

Calculating the effective permeability K_{eff} in different REV size.

The largest sample used had an edge length of 3 mm and consisted of 1051 cells. A smaller sample with an edge length of 2 mm was extracted from the center of the 3 mm sample, and so on until samples with an edge length of 1 mm and 0.5 mm were also obtained (Figure A). A thick cell wall was generated due to the limited resolution of the X-ray micro-CT (voxel size = 8.5 µm). Image erosion and subsequent geometrical algorithms presented in Section 2.1.1 only worked for voxel erosion of more than three voxels. Hence, the resulting cell wall thickness was around 25 µm. For apple tissue, the cell wall thickness is in the range of 1 to 10 µm (1–3). As the main purpose of this REV analysis was to compare the permeability of different sample sizes, the realistic cell wall thickness was not required. Steady-state simulation of water transport was done in each of the REVs, by setting up the water activity at 0.98 (turgid condition), so no deformation. The comparison of microstructural components and the calculated effective permeability are presented in Table 3.

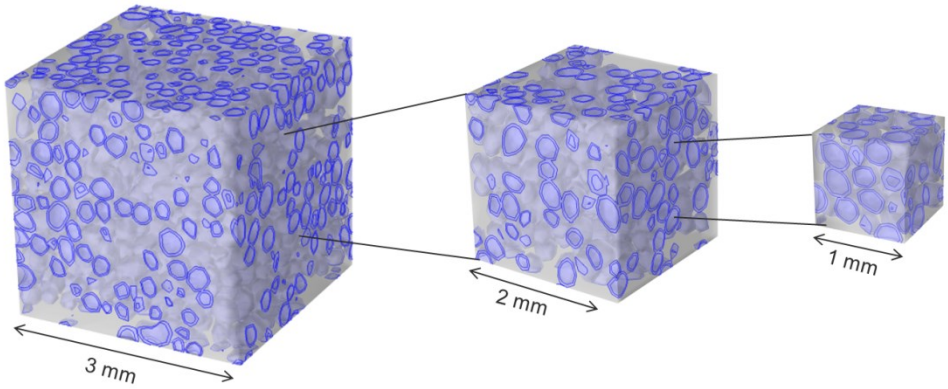

Figure A. Tissue sample used for determining the Representative Elementary Volume (REV). A cubical tissue with an edge length of 3 mm was divided into smaller tissue (2 mm, 1 mm and 0.5 mm). The protoplast and cell wall domains are highlighted in blue.

Supplementary material B

Comparison between experiments and simulations with a multiscale approach

Results of the macroscale modeling using the upscaled moisture transport properties are compared with experimental data of (4) to check the reliability and accuracy of the upscaling approach. The free shrinkage case shows a good agreement in terms of the water content, especially during the first 10 hours of drying, although the drying rate was a bit higher (Figure B a and b). The lysis case, however, overpredicts the drying rate that gives a relatively fast moisture removal at the first 7 hours. These differences can be understood since the experimental procedure of (4) did not include any steps to promotes lysis. The cells may undergo lysis naturally at some point during drying, but the analysis of the occurrence was not the focus of the experiment. The tissue temperature decreases due to the evaporative cooling effect as the water is removed from the tissue surface. The two simulation cases exhibit a lower core temperature during the first 10 hours of drying compared to the experimental data. The differences are in the range of 1 – 2 °C. The faster drying rate induces larger effect of evaporative cooling. In the simulations, the core temperature reaches the wet-bulb temperature of 14.75°C. It is the minimum temperature that can be attained at the given drying conditions (T = 23°C and RH = 40%).

In general, some discrepancies are found between the experimental data and simulation results. They can be explained by two reasons. Firstly, the moisture transport properties of the sample in the experiment are not the same as the upscaled properties used in macroscale modeling. Biological variabilities exist between individual fruit due to the type of cultivar, ripeness level, cultivation sites or harvest year, etc. In the context of microscale modeling, the biological variability results in differences in porosity, cell size, cell wall thickness, membrane permeability, among others. These could affect the calculated upscaled properties. Secondly, the discrepancies may come from the unmodeled physics at a later stage of drying. As it is shown in other studies (5,6), porous layers are formed during drying as a result of cell wall stiffening due to moisture removal. In this case, the moisture transfer mechanism changes from a liquid diffusion-dominated mechanism through the cell wall to vapor diffusion-dominated mechanism through the pores. Furthermore, the decreasing shrinkage rate at this drying stage makes the moisture path to reach the tissue surface longer. This phenomenon is not captured by the microscale model and it will overpredict the effective permeability of the tissue. As a result, the drying rate is higher in the simulation especially between three until seven hours of drying. Nevertheless, the macroscale modeling using the upscaled properties gives adequate matches with the experimental data where the drying rates and temperature are still in the same order of magnitude.

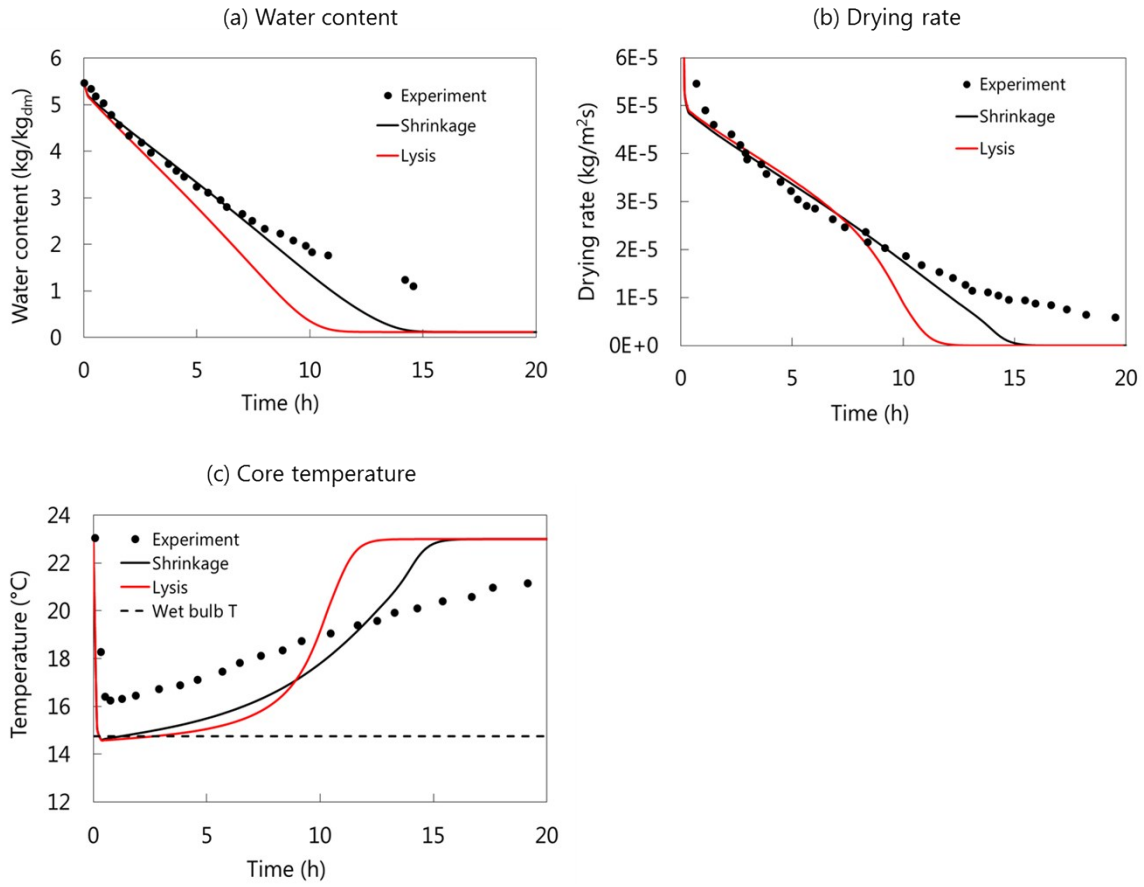

Figure B. Comparison between the macroscale simulation and experimental results of (4): (a) water content, (b) drying rate and (c) core temperature. Two dehydration cases are considered in the simulations, namely free shrinkage and total lysis.

References

1. Ben-Arie R, Kislev N, Frenkel C. Ultrastructural changes in the cell walls of ripening apple and pear fruit. Plant Physiol. 1979;64(2)(2):197–202.
2. Mebatsion HK, Verboven P, Melese Endalew A, Billen J, Ho QT, Nicolaï BM. A novel method for 3-D microstructure modeling of pome fruit tissue using synchrotron radiation tomography images. J Food Eng [Internet]. 2009;93(2):141–8. Available from: http://dx.doi.org/10.1016/j.jfoodeng.2009.01.008
3. Joardder MUH, Brown RJ, Kumar C, Karim MA. Effect of Cell Wall Properties on Porosity and Shrinkage of Dried Apple. Int J Food Prop [Internet]. 2015;18(10):2327–37. Available from: http://www.tandfonline.com/doi/full/10.1080/10942912.2014.980945
4. Defraeye T, Verboven P. Convective drying of fruit: role and impact of moisture transport properties in modelling. J Food Eng [Internet]. 2016;193:95–107. Available from: http://dx.doi.org/10.1016/j.jfoodeng.2016.08.013
5. Karathanos VT, Kanellopoulos NK, Belessiotis VG. Development of porous structure during air drying of agricultural plant products. J Food Eng [Internet]. 1996 Aug;29(2):167–83. Available from: https://www.sciencedirect.com/science/article/pii/0260877495000585
6. Madiouli J, Sghaier J, Lecomte D, Sammouda H. Determination of porosity change from shrinkage curves during drying of food material. Food Bioprod Process [Internet]. 2012;90(1):43–51. Available from: http://dx.doi.org/10.1016/j.fbp.2010.12.002